

# $K^+$ -nucleus elastic scattering revisited from perspective of partial restoration of chiral symmetry

Kenji Aoki\* and Daisuke Jido

*Department of Physics, Tokyo Metropolitan University, Hachioji, Tokyo 192-0397, Japan \*E-mail: aoki-kenji1@ed.tmu.ac.jp*

.....  
The  $K^+$  meson properties in the nuclear medium are investigated by considering the wavefunction renormalization as a first step to reveal the in-medium properties of the  $K^+$  meson in the context of partial restoration of chiral symmetry. The  $K^+N$  elastic scattering amplitude is constructed using chiral perturbation theory up to the next-to-leading order. Using the constructed amplitude, we calculate the wavefunction renormalization in the Thomas-Fermi approximation. We obtained a good description of the  $K^+N$  elastic scattering amplitude. The obtained wavefunction renormalization factor suggests the 5 to 8% enhancement of the  $K^+N$  interaction at the saturation density. We conclude that the wavefunction renormalization could be one of the important medium effects for the  $K^+$  meson.  
.....

Subject Index      D33, D32, B60, B69

## 1. Introduction

The strong interaction properties of hadron in the nuclear medium has attracted considerable interests, in particular, for the purpose of proving the spontaneous breaking of chiral symmetry from the experimental facts. The spontaneous breaking of chiral symmetry is considered to be one of the phase transition phenomena in the Quantum Chromodynamics (QCD) vacuum. Thus, by changing the temperature and/or density of the system, one expects that the broken symmetry might be restored. With this nature, we try to prove the mechanism of the spontaneous breaking of chiral symmetry from the experimental facts. In the phase transition of the QCD vacuum, the quark condensate  $\langle \bar{q}q \rangle$  is one of the order parameters that characterize chiral symmetry breaking. At high temperature and/or high density, the magnitude of the quark condensate is considered to be decreasing. Especially, in the finite density and zero temperature system, such as atomic nuclei, chiral symmetry is considered to be partially restored and the magnitude of the quark condensate is sufficiently reduced. So, we study the partial restoration of chiral symmetry, which may be more easily accessible situation than the complete restoration of chiral symmetry at extreme conditions, in order to prove the mechanism of the spontaneous breaking of chiral symmetry. For this purpose, we study the behavior of the quark condensate in the nuclear medium. However, since the quark condensate is not a direct observable quantity, one is forced to extract the information of the quark condensate indirectly by analyzing the experimental observables, such as hadron-nucleus scattering. Suitable systems for such studies may be Nambu-Goldstone (NG) bosons in the nuclear medium, because the NG bosons should be sensitive to the spontaneous

---

breaking of chiral symmetry and the NG bosons change their properties in nuclear medium. Comparing in-medium and in-vacuum NG boson properties quantitatively, one may prove the reduction of the magnitude of the quark condensate quantitatively from the observations.

The study of the partial restoration of chiral symmetry have been carried out especially for pion. From the observations of the deeply bound pionic atom [1] and low-energy pion-nucleus elastic scattering [2] taking into accounts the theoretical considerations [3, 4], chiral symmetry is considered to be restored about 30% at the saturation density. So, systematic studies for other systems are necessary, and we need to confirm consistency of partial restoration of chiral symmetry in other systems. Yet, we do not know whether the partial restoration of chiral symmetry systematically occurs in other than pion-nucleus systems. For this purpose, we would like to consider the NG bosons with strangeness.

The promising proves to investigate the nature of the strangeness in nuclear medium are  $K^\pm$ . It is known that the strong interaction properties of  $K^+$  and  $K^-$  with nucleon, or with nuclei, are considerably different due to their strangeness content [5]. It is assigned that  $S = +1$  for  $K^+$  and  $S = -1$  for  $K^-$ . We know that  $\bar{K}N$  interaction is so strong attractive that  $\Lambda(1405)$  has been considered to appear as a quasi bound state of  $\bar{K}N$  [6]. When we consider the  $\bar{K}$ -nucleus system, strong absorption into the nucleus masks medium effects on the  $\bar{K}$  meson. On the other hand, the  $K^+N$  interaction in vacuum is repulsive and relatively weak in the low-energy region  $p_{\text{lab}} \leq 800$  MeV/c where inelasticity is small. The  $K^+N$  cross section is small in comparison with  $K^-N$  and the mean free path in nuclear medium is long and comparable to the typical nuclear size 5-7 fm. Further, there is no hyperon resonances strongly coupled to  $K^+N$ . With this nature, the  $K^+$  meson can penetrate deeply in the nucleus without suffering from the strong absorption. Therefore, it is suggested that the  $K^+$  meson is capable of using as good probe to investigate the nature of the strangeness in nuclear medium.

Based on the fact that the mean free path of the  $K^+$  meson in nuclear medium is comparable to the typical nuclear size, one would consider that the  $K^+$  meson scattering with nucleons in the nucleus could be described by the single step scattering, that is the linear density approximation would be valid. It is remarkable that the ratio  $R$  of the total elastic cross section for  $K^+$ -carbon on the total elastic cross section for  $K^+$ -deuteron per nucleon is given by

$$R = \frac{\sigma(K^+ {}^{12}\text{C})}{6\sigma(K^+ d)} > 1 \quad (1)$$

in the region of kaon lab momenta  $p_{\text{lab}} = 450\text{-}900$  MeV/c [7-9]. By the expectation of the in-vacuum  $K^+N$  interaction, the  $K^+$ -carbon scattering would satisfy the linear density approximation, namely  $\sigma(K^+ {}^{12}\text{C}) \simeq 12\sigma(K^+ N)$ . However, Eq. (1) suggests that the single-step scattering does not explain the elastic total cross section for  $K^+$ -carbon scattering. Even, the ratio should be expected as rather  $R < 1$  if one considers the nuclear shadowing effect. This observation was also found as breakdown of the low-density  $T\rho$  approximation in the  $K^+$  optical potential in nuclei extracted from data of  $K^+$ -nucleus elastic scatterings [10]. The study of Ref. [10] tells us that the optical potential which reproduces the experimental data for the  $K^+$ -nucleus elastic scattering is 14-34% enhanced than what one expects from a simple  $T\rho$  approximation.

---

To understand such unanticipated enhancement of the  $K^+N$  interaction in nuclear medium, several ideas have been proposed. As unconventional in-medium effects, the “swelling” of nucleons in nuclei was firstly suggested in Ref. [11] and later in Ref. [12]. The model which could provide the physical interpretation of the “swelling” was proposed in Ref. [13] considering the reduction of the mass of the vector meson, which intermediates the effective  $K^+N$  interaction, in the nuclear medium. Other possibilities were discussed, for instance, by considering the medium corrections on the meson exchange current [14], by including pion cloud contribution [15] and by putting medium effects on exchanged mesons between the  $K^+$  and the target nucleons [16]. The recent studies using the optical potential based on the in-medium kinematics were done in Ref. [17, 18].

In this paper, we would like to describe the enhancement of the  $K^+N$  interaction in the nuclear medium in terms of the wavefunction renormalization of the in-medium kaon [19]. The wavefunction renormalization should be taken into account, if the self-energy has energy-dependence. The self-energy for the NG boson is expected to have substantial energy dependence, because, according to the chiral effective theory, the amplitude is written in terms of the derivative expansion of the NG boson field. Thus, we expect that the wavefunction renormalization plays a crucial role as of the leading-order corrections to the  $K^+N$  interaction. In addition, the wavefunction renormalization is intimately connected to partial restoration of chiral symmetry [3, 4, 20], which provides one of the fundamental interpretations of the in-medium properties of hadron. In the chiral effective theory, the NG boson field is introduced as a parametrization of the coset space of the broken symmetry, and thus should be normalized by a dimensional quantity because the physical boson field has mass dimension while the field parametrizing the coset space is dimensionless. Once partial restoration of chiral symmetry takes places in nuclear matter by reduction of the chiral order parameters, it changes the energy scale of the vacuum and renormalizes the NG boson field. For these reasons, we would like to examine the wavefunction renormalization of the in-medium  $K^+$  using the in-vacuum  $K^+N$  elastic scattering amplitude calculated from chiral perturbation theory and its unitarization. This study can be a first step to describe the in-medium  $K^+$  property by more systematic approaches, such as in-medium chiral perturbation theory.

This paper is organized as follows. In Sec. 2, we summarize the model of the in-medium kaon self-energy and investigate the properties of the wavefunction renormalization. In Sec. 3, we describe the formulation of chiral perturbation theory and calculate the in-vacuum  $K^+N$  amplitude. In Sec. 4, we discuss the numerical results. The total cross section and differential cross section of the  $K^+N$  elastic scattering are presented. We discuss the wavefunction renormalization. In Sec. 5, we conclude the results of this paper.

## 2. Wavefunction renormalization

As stated in introduction, the aim of this paper is to describe the role of the wavefunction renormalization in the in-medium  $K^+$  self-energy, that is the optical potential for  $K^+$  in the nuclear medium. For this purpose, we take a simple description of the  $K^+$  self-energy based on the  $K^+N$  elastic scattering amplitude:

$$\Pi(\omega, \vec{p}) = 4 \int^{k_F} \frac{d^3q}{(2\pi)^3 2M_N} T_{K^+N}(p, q) \quad (2)$$

where  $T_{K+N}(p, q)$  is the forward elastic  $K^+N$  scattering amplitude with kaon momentum  $p$  and nucleon momentum  $q$  and is integrated with respect to the nucleon spacial momentum up to the Fermi momentum  $k_F = (3\pi^2\rho/2)^{1/3}$ . Here we consider the isospin symmetric nuclear matter. The factor 4 is the multiplicity of the spin and isospin. The bound nucleons in the nuclear medium are described by Thomas-Fermi approximation in which the nucleons are treated as Fermi gas in a potential  $v_N = -k_F^2/2M_N$  and the energy of the nucleon with momentum  $q$  is given by  $E_N = M_N + q^2/2M_N + v_N$ . Here the nucleon spinor is normalized as  $\bar{u}(q, s)u(q, s') = 2M_N\delta_{ss'}$ . The scattering amplitude  $T_{K+N}(p, q)$  is evaluated in the nuclear matter rest frame and is allowed to extend to the energy region off the mass shell of  $K^+$  according to chiral perturbation theory. The off-shell extension is necessary to calculate the wavefunction renormalization, which is obtained by partial derivative of the self-energy with respect to the  $K^+$  energy by fixing the momentum. The description of the  $K^+N$  scattering amplitude will be given in the next section. If one neglects Fermi motion of the nucleons in the nuclear matter, one finds that Eq. (2) is reduced to the  $T\rho$  approximation

$$\Pi(\omega, \vec{p}) = \rho T_{K+N}(\omega, \vec{p}). \quad (3)$$

Let us consider the case that the  $K^+$  self-energy in the nuclear medium should have energy dependence. In such a case, the effect of the energy dependence can be implemented to an equivalent energy independent self-energy at the  $K^+$  pole with the wavefunction renormalization factor as follows. Following the discussion for the  $\pi$  meson in Ref. [3], we introduce the Klein-Gordon equation for the in-medium  $K^+$  with energy  $\omega^*$ , momentum  $\vec{p}$  and the in-vacuum mass  $M_K$  as

$$\omega^{*2} - \omega^2 - \Pi(\omega^*, \vec{p}) = 0 \quad (4)$$

with  $\omega = \sqrt{\vec{p}^2 + M_K^2}$  and the self-energy  $\Pi(\omega^*, \vec{p})$ . Here let us assume that  $\Pi(\omega^*) \ll \omega^2$ , which means that the one-body potential for  $K^+$  produced by the nuclear medium is sufficiently small in comparison with the free kaon energy, so that the effects of the self-energy to the free  $K^+$  meson is considered to be moderately small,  $\omega^* \simeq \omega$ . With this assumption, expanding the self-energy around  $\omega^* = \omega$  and evaluating it at the on-shell condition Eq. (4) with  $\omega^* = \omega$ , we obtain

$$\begin{aligned} \Pi(\omega^*) &= \Pi(\omega) + (\omega^{*2} - \omega^2) \left. \frac{\partial \Pi}{\partial \omega^{*2}} \right|_{\omega^*=\omega} + \dots \\ &\simeq \left( 1 + \left. \frac{\partial \Pi}{\partial \omega^{*2}} \right|_{\omega^*=\omega} \right) \Pi(\omega) \equiv Z \Pi(\omega), \end{aligned} \quad (5)$$

$$Z \equiv 1 + \left. \frac{\partial \Pi}{\partial \omega^{*2}} \right|_{\omega^*=\omega} \quad (6)$$

where we neglect the higher orders of  $(\omega^{*2} - \omega^2)$  and in the second line we assume that the difference between  $\Pi(\omega^*)$  and  $\Pi(\omega)$  is in higher orders in density expansion. Here we have introduced the wavefunction renormalization factor as  $Z$ . Therefore, when the self-energy has sufficiently strong energy-dependence, which may be the case for the NG bosons, the wavefunction renormalization plays an important role as one of the substantial in-medium effects.

In the present model, the self-energy is given by the  $K^+N$  scattering amplitude as shown in Eq. (2). Thus, the wavefunction renormalization factor  $Z$  is obtained from the  $K^+$  energy

dependence of the scattering amplitude. In the leading order of the density expansion, the in-medium self-energy is given by the  $T\rho$  approximation Eq. (3). Thus, the wavefunction renormalization is one of the next-to-leading corrections for the in-medium self-energy. (The leading correction is given by the in vacuum  $K^+N$  scattering amplitude.) Here we would like to emphasize that the wavefunction renormalization is the leading order correction to the  $K^+N$  interaction. In the following sections, we describe the  $K^+N$  scattering amplitude based on chiral perturbation theory and see whether the wavefunction renormalization explains the enhancement of the  $K^+N$  interaction in the nuclear medium.

### 3. Formulation for $K^+N$ amplitudes

In this section we describe the  $KN$  elastic scattering amplitude. We calculate the  $KN$  scattering amplitude at tree level based on chiral perturbation theory up to the next-to-leading order. Then, we also see the unitarized amplitude of the tree amplitude by following the method developed for the  $\bar{K}N$  scattering where the  $\Lambda(1405)$  is dynamically generated [6, 21–23]. We determine the low energy constants appearing in the next-to-leading order so as to reproduce the observed  $K^+N$  differential cross sections at certain momentum. To compare the calculated amplitude with the observation, we take into the Coulomb correction, which becomes important especially for the forward scattering, to the  $K^+p$  amplitude.

#### 3.1. Chiral perturbation theory

We use chiral perturbation theory as a low energy effective theory of QCD to describe the  $K^+N$  interaction. Chiral perturbation theory which has  $SU(3)_L \times SU(3)_R$  symmetry describes interaction between the pseudoscalar Nambu-Goldstone bosons and  $1/2^+$  baryon octet. The leading order chiral lagrangian is given for the baryon field  $B$  as

$$\mathcal{L}_{MB}^{(1)} = \text{Tr} [\bar{B}(i \not{D} - M_0)B] - \frac{D}{2} \text{Tr} (\bar{B} \gamma_\mu \gamma_5 \{u^\mu, B\}) - \frac{F}{2} \text{Tr} (\bar{B} \gamma_\mu \gamma_5 [u^\mu, B]), \quad (7)$$

where  $M_0$  is the baryon mass at the chiral limit, and

$$D_\mu B = \partial_\mu B + [\Gamma_\mu, B], \quad (8)$$

$$\Gamma_\mu = \frac{1}{2}(\xi^\dagger \partial_\mu \xi + \xi \partial_\mu \xi^\dagger), \quad (9)$$

$$U = \xi^2 = \exp \left( i \frac{\sqrt{2}}{f} \Phi \right), \quad (10)$$

$$u_\mu = i \left( \xi^\dagger \partial_\mu \xi - \xi \partial_\mu \xi^\dagger \right). \quad (11)$$

The constants  $D$  and  $F$  give the axial vector couplings of the baryons at tree level. The meson and baryon fields form the  $SU(3)$  matrix given by

$$\Phi = \begin{pmatrix} \frac{\pi^0}{\sqrt{2}} + \frac{\eta}{\sqrt{6}} & \pi^+ & K^+ \\ \pi^- & -\frac{\pi^0}{\sqrt{2}} + \frac{\eta}{\sqrt{6}} & K^0 \\ K^- & \bar{K}^0 & -\frac{2\eta}{\sqrt{6}} \end{pmatrix}, \quad (12)$$

$$B = \begin{pmatrix} \frac{\Sigma^0}{\sqrt{2}} + \frac{\Lambda}{\sqrt{6}} & \Sigma^+ & p \\ \Sigma^- & -\frac{\Sigma^0}{\sqrt{2}} + \frac{\Lambda}{\sqrt{6}} & n \\ \Xi^- & \Xi^0 & -\frac{2\Lambda}{\sqrt{6}} \end{pmatrix}. \quad (13)$$

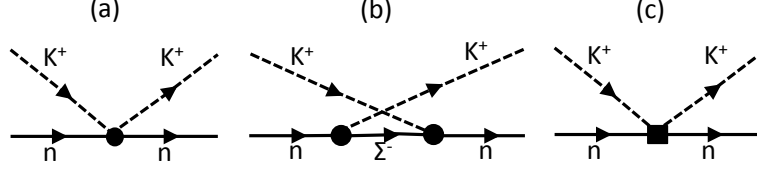


**Fig. 1** Feynman diagrams for  $K^+n$  elastic scattering. (a) Weinberg-Tomozawa interaction. (b) Crossed Born interaction with the intermediate  $\Sigma^-$ . (c) NLO interaction.

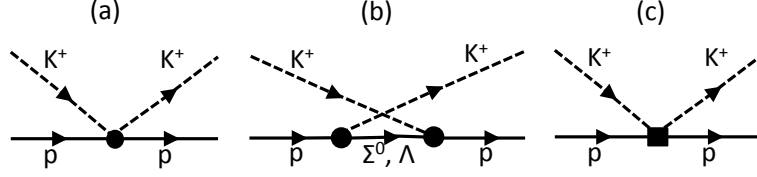


**Fig. 2** Feynman diagrams for  $K^+p$  elastic scattering. (a) Weinberg-Tomozawa interaction. (b) Crossed Born interaction with the intermediate  $\Sigma^0$  or  $\Lambda$ . (c) NLO interaction.

The next-to-leading order chiral lagrangian reads

$$\begin{aligned} \mathcal{L}_{MB}^{(2)} = & b_D \text{Tr}(\bar{B}\{\chi_+, B\}) + b_F \text{Tr}(\bar{B}[\chi_+, B]) + b_0 \text{Tr}(\bar{B}B) \text{Tr}(\chi_+) \\ & + d_1 \text{Tr}(\bar{B}\{u_\mu[u^\mu, B]\}) + d_2 \text{Tr}(\bar{B}[u_\mu, [u^\mu, B]]) + d_3 \text{Tr}(\bar{B}u_\mu) \text{Tr}(u^\mu B) \\ & + d_4 \text{Tr}(\bar{B}B) \text{Tr}(u^\mu u_\mu), \end{aligned} \quad (14)$$

with

$$\chi_+ = 2B_0 \left( \xi \mathcal{M} \xi + \xi^\dagger \mathcal{M} \xi^\dagger \right), \quad (15)$$

$$\mathcal{M} = \text{diag}(\hat{m}, \hat{m}, m_s), \quad (16)$$

where  $b_D, b_F, b_0, d_1, d_2, d_3$  and  $d_4$  are the low-energy constants. We assume the isospin symmetry and  $\hat{m} \equiv (m_u + m_d)/2$  is the isospin averaged value of the current quark masses. The parameter  $B_0$  is a positive constant connected to the meson mass. In this work, the parameter  $B_0$  is fixed by  $B_0 = M_K^2/(\hat{m} + m_s)$  where  $M_K$  is the  $K$  meson mass. The low-energy constants in the next-to-leading order chiral lagrangian are determined by the  $K^+N$  elastic cross section and the baryon masses. The baryon masses at the next-to-leading order are given by

$$M_\Sigma = M_0 - 4B_0 [2b_D \hat{m} + b_0(2\hat{m} + m_s)], \quad (17)$$

$$M_\Xi = M_0 - 4B_0 [b_D(\hat{m} + m_s) + b_F(m_s - \hat{m}) + b_0(2\hat{m} + m_s)], \quad (18)$$

$$M_N = M_0 - 4B_0 [b_D(\hat{m} + m_s) + b_F(\hat{m} - m_s) + b_0(2\hat{m} + m_s)], \quad (19)$$

$$M_\Lambda = M_0 - 4B_0 \left[ b_D \frac{2(\hat{m} + m_s)}{3} + b_0(2\hat{m} + m_s) \right]. \quad (20)$$

For the  $K^+n$  elastic scattering, the Feynman diagrams to be calculated are shown Fig. 1. The direct Born term does not contribute, since there is no baryon resonance with

strangeness  $S = 1$ . The pentaquark  $\Theta^+$  can be a candidate for the direct Born term. But here we do not take into account, because it is known that the possible  $\Theta^+$  has very weak coupling to  $K^+N$ . In the crossed Born term, the intermediate state has  $S = -1$  and  $Q = -1$ , and the candidate baryon is the  $\Sigma^-$  baryon. It turns out to give small contribution. The  $K^+n$  invariant amplitudes at the leading order chiral perturbation theory are calculated as

$$T_{\text{WT}}^{K^+n} = \frac{1}{4f_K^2} \bar{u}(\vec{p}_4, s_4) (\not{p}_1 + \not{p}_3) u(\vec{p}_2, s_2), \quad (21)$$

$$T_{\text{Born}}^{K^+n} = -\frac{(D-F)^2}{2f_K^2} \bar{u}(\vec{p}_4, s_4) \not{p}_1 \gamma_5 \frac{M_\Sigma + (\not{p}_2 - \not{p}_3)}{M_\Sigma^2 - (p_2 - p_3)^2 - i\epsilon} \not{p}_3 \gamma_5 u(\vec{p}_2, s_2), \quad (22)$$

where the constants  $M_\Sigma$  and  $f_K$  are the sigma baryon mass and kaon decay constant, respectively, with the initial kaon momentum  $p_1$ , the initial nucleon momentum  $p_2$ , the final kaon momentum  $p_3$  and the final nucleon momentum  $p_4$ .  $u(\vec{p}_i, s_i)$  is positive energy Dirac spinor for the 3-momentum  $\vec{p}_i$  and spin  $s_i$ . Equations (21) and (22) are obtained from Weinberg-Tomozawa interaction and crossed Born interaction, respectively. The  $K^+n$  invariant amplitude at the next-to-leading order chiral perturbation theory is calculated as

$$T_{(2)}^{K^+n} = \left[ \frac{2B_0}{f_K^2} (\hat{m} + m_s) (2b_0 + b_D - b_F) + \frac{2}{f_K^2} (d_1 - d_2 - 2d_4) (p_1 p_3) \right] \bar{u}(\vec{p}_4, s_4) u(\vec{p}_2, s_2). \quad (23)$$

For the  $K^+p$  elastic scattering, we calculate the Feynman diagrams shown in Fig. 2. Since there is no baryon with  $S = 1$  and  $Q = 2$ , we have no direct Born terms. In the crossed Born term, the  $\Sigma^0$  baryon and  $\Lambda$  baryon are possible intermediate one particle states with  $S = -1$  and  $Q = 0$ . The  $K^+p$  invariant amplitude at the leading order chiral perturbation theory is obtained as

$$T_{\text{WT}}^{K^+p} = \frac{1}{2f_K^2} \bar{u}(\vec{p}_4, s_4) (\not{p}_1 + \not{p}_3) u(\vec{p}_2, s_2), \quad (24)$$

$$\begin{aligned} T_{\text{Born}}^{K^+p} = & -\left( \frac{D-F}{2f_K} \right)^2 \bar{u}(\vec{p}_4, s_4) \not{p}_1 \gamma_5 \frac{M_\Sigma + (\not{p}_2 - \not{p}_3)}{M_\Sigma^2 - (p_2 - p_3)^2 - i\epsilon} \not{p}_3 \gamma_5 u(\vec{p}_2, s_2) \\ & -\left( \frac{3F+D}{2\sqrt{3}f_K} \right)^2 \bar{u}(\vec{p}_4, s_4) \not{p}_1 \gamma_5 \frac{M_\Lambda + (\not{p}_2 - \not{p}_3)}{M_\Lambda^2 - (p_2 - p_3)^2 - i\epsilon} \not{p}_3 \gamma_5 u(\vec{p}_2, s_2) \end{aligned} \quad (25)$$

with the  $\Lambda$  mass  $M_\Lambda$ . The  $K^+p$  invariant amplitude at the next-to-leading order chiral perturbation theory is calculated as

$$T_{(2)}^{K^+p} = \left[ \frac{4B_0}{f_K^2} (\hat{m} + m_s) (b_0 + b_D) - \frac{2}{f_K^2} (2d_2 + d_3 + 2d_4) (p_1 p_3) \right] \bar{u}(\vec{p}_4, s_4) u(\vec{p}_2, s_2). \quad (26)$$

The  $K^+N$  scattering amplitudes in the particle basis,  $T^{K^+p}$  and  $T^{K^+n}$ , are decomposed into the amplitude in the isospin basis  $T^I$  ( $I = 0, 1$ ) as

$$T^{K^+p} = T^{I=1}, \quad (27)$$

$$T^{K^+n} = \frac{1}{2} (T^{I=1} + T^{I=0}). \quad (28)$$

We work out in the center of mass (c.m.) frame, where we perform the partial wave decomposition. In the c.m. frame the invariant amplitude  $T^I$  is written by the non spin-flip and

spin-flip amplitudes,  $f^I$  and  $g^I$ , as

$$T^I(s, \theta_{\text{c.m.}}) = f^I(s, \theta_{\text{c.m.}}) - i\vec{\sigma} \cdot \hat{n} g^I(s, \theta_{\text{c.m.}}) \quad (29)$$

as functions of the Mandelstam variable  $s$  and the scattering angle  $\theta_{\text{c.m.}}$  in the c.m. frame, where  $\vec{\sigma}$  is the spin Pauli matrix and the normal vector  $\hat{n}$  of the scattering plane given by

$$\hat{n} = \frac{\vec{k}' \times \vec{k}}{|\vec{k}' \times \vec{k}|} \quad (30)$$

with the incident and scattered kaon momenta,  $\vec{k}$  and  $\vec{k}'$ .

The differential cross section for the  $K^+N$  elastic scattering in the c.m. frame is given by

$$\frac{d\sigma(K^+N)}{d\Omega} = \frac{1}{64\pi^2 s} (|f^{K^+N}|^2 + |g^{K^+N}|^2). \quad (31)$$

The total cross section in the c.m. frame for isospin  $I$  is obtained by integrating the differential cross section in terms of the solid angle  $d\Omega = \sin\theta_{\text{c.m.}} d\theta_{\text{c.m.}} d\phi$

$$\sigma^I = \frac{1}{64\pi^2 s} \int d\Omega (|f^I|^2 + |g^I|^2). \quad (32)$$

The amplitudes,  $f^I$  and  $g^I$ , are expanded into the partial waves with Legendre polynomials  $P_l(x)$  as

$$\begin{aligned} f^I(s, \theta_{\text{c.m.}}) &= \sum_{l=0}^{\infty} f_l^I(s) P_l(\cos\theta_{\text{c.m.}}) \\ &= \sum_{l=0}^{\infty} [(l+1)T_{l+}^I(s) + lT_{l-}^I(s)] P_l(\cos\theta_{\text{c.m.}}), \end{aligned} \quad (33)$$

$$\begin{aligned} g^I(s, \theta_{\text{c.m.}}) &= \sum_{l=1}^{\infty} g_l^I(s) \sin\theta_{\text{c.m.}} \frac{dP_l(\cos\theta_{\text{c.m.}})}{d\cos\theta_{\text{c.m.}}} \\ &= \sum_{l=1}^{\infty} [T_{l+}^I(s) - T_{l-}^I(s)] \sin\theta_{\text{c.m.}} \frac{dP_l(\cos\theta_{\text{c.m.}})}{d\cos\theta_{\text{c.m.}}}, \end{aligned} \quad (34)$$

where we have introduced the partial wave amplitudes,  $T_{l\pm}^I(s)$ , which have definite total angular momentum. For lower partial waves, the explicit relation of these two amplitudes are found as

$$T_{0+}^I = f_{l=0}^I, \quad (35)$$

$$T_{1+}^I = \frac{1}{3} (f_{l=1}^I + g_{l=1}^I), \quad (36)$$

$$T_{1-}^I = \frac{1}{3} (f_{l=1}^I - 2g_{l=1}^I), \quad (37)$$

$$T_{2+}^I = \frac{1}{5} (f_{l=2}^I + 2g_{l=2}^I), \quad (38)$$

$$T_{2-}^I = \frac{1}{5} (f_{l=2}^I - 3g_{l=2}^I) \quad (39)$$

and so on.

As we have seen above, in our formulation, we carry out the partial wave decomposition in the c.m. frame. The self-energy Eq. (2), however, is calculated in the rest frame of the



nuclear medium, in which each nucleon has its own Fermi motion. Thus, we need the  $K^+N$  amplitude beyond the c.m. frame. Although the amplitudes obtained in the c.m. frame can be written in terms of the Lorentz invariant amplitudes which are available in any Lorentz frame, we perform the partial wave decomposition and unitarization in the c.m. frame. For this reason, we have to evaluate the  $K^+N$  amplitude in the c.m. frame and make Lorentz transformation from the nuclear matter rest frame to the  $K^+N$  c.m. frame.

### 3.2. Coulomb corrections

For the  $K^+p$  scattering, we take into account the Coulomb correction to compare the amplitude calculated theoretically to the observed differential cross section. By following Ref. [24], we add the Coulomb amplitude  $f_C$  to the strong interaction part of the  $K^+p$  scattering multiplied by the Coulomb phase shift factor  $e^{2i\Phi_l}$ :

$$f^{K^+p} = \sum_{l=0}^{\infty} [(l+1)\mathcal{T}_{l+}^{I=1} + l\mathcal{T}_{l-}^{I=1}] e^{2i\Phi_l} P_l(\cos \theta_{\text{c.m.}}) - 8\pi\sqrt{s}f_C, \quad (40)$$

$$g^{K^+p} = \sum_{l=1}^{\infty} [\mathcal{T}_{l+}^{I=1} - \mathcal{T}_{l-}^{I=1}] e^{2i\Phi_l} \sin \theta_{\text{c.m.}} \frac{dP_l(\cos \theta_{\text{c.m.}})}{d \cos \theta_{\text{c.m.}}}. \quad (41)$$

The Coulomb amplitude and Coulomb phase shift are described as

$$f_C = \frac{\alpha}{2kv \sin^2(\theta/2)} \exp \left[ -i \frac{\alpha}{v} \ln \left( \sin^2 \frac{\theta}{2} \right) \right], \quad (42)$$

$$\Phi_l = \sum_{n=1}^l \tan^{-1} \frac{\alpha}{nv} \quad (43)$$

for  $l > 0$  ( $\Phi_0=0$ ) with the relative velocity between the kaon and proton  $v$

$$v = \frac{k(E_K + E_p)}{E_K E_p}, \quad (44)$$

where  $E_K$  and  $E_p$  are the kaon energy and proton energies in the c.m. system, respectively and  $\alpha$  is the fine structure constant.

### 3.3. Unitarization

In this subsection, we carry out the unitarization of the scattering amplitude calculated by chiral perturbation theory. By carrying out the unitarization, we can obtain scattering amplitude as a complex function consistent with elastic unitarity and we can extend energy applicable region. For the unitarization, one performs non-perturbative algebraic summation of specific diagrams using the tree level chiral perturbation theory as a potential kernel so as to satisfy the elastic unitarity. We work out in the isospin basis in which we decompose the  $K^+N$  amplitude into the isospin 0 and 1, and carry out the unitarization in each partial waves following the method developed in Ref. [25].

We perform the unitarization for each partial wave amplitude  $T_{l\pm}^I$  by solving the Lippmann-Schwinger equation

$$T_{l\pm}^I = V_{l\pm}^I + V_{l\pm}^I G T_{l\pm}^I. \quad (45)$$

This equation can be solved as an algebraic equation after the on-shell factorization with the  $N/D$  method [23, 26],

$$\begin{aligned}\mathcal{T}_{l\pm}^I &= V_{l\pm}^I + V_{l\pm}^I G V_{l\pm}^I + V_{l\pm}^I G V_{l\pm}^I G V_{l\pm}^I + \dots \\ &= \frac{V_{l\pm}^I}{1 - V_{l\pm}^I G}.\end{aligned}\quad (46)$$

We make good use of the tree level amplitudes obtained with chiral perturbation theory for the interaction kernel of the scattering equation after making the partial wave decomposition of

$$V^I = T_{\text{WT}}^I + T_{\text{Born}}^I + T_{(2)}^I. \quad (47)$$

The loop function  $G$  is defined as

$$G = i \int \frac{d^4 q}{(2\pi)^4} \frac{1}{(P - q)^2 - M_N^2 + i\epsilon} \frac{1}{q^2 - M_K^2 + i\epsilon}. \quad (48)$$

The loop function can be calculated with the dimensional regularization as

$$\begin{aligned}G &= \frac{1}{(4\pi)^2} \left\{ a(\mu) + \ln \frac{M_N^2}{\mu^2} + \frac{M_K^2 - M_N^2 + s}{2s} \ln \frac{M_K^2}{M_N^2} \right. \\ &\quad + \frac{\bar{q}}{\sqrt{s}} \left[ \ln(s - (M_N^2 - M_K^2) + 2\sqrt{s}\bar{q}) + \ln(s + (M_N^2 - M_K^2) + 2\sqrt{s}\bar{q}) \right. \\ &\quad \left. \left. - \ln(-s + (M_N^2 - M_K^2) + 2\sqrt{s}\bar{q}) - \ln(-s - (M_N^2 - M_K^2) + 2\sqrt{s}\bar{q}) \right] \right\} \quad (49)\end{aligned}$$

where the parameter  $a(\mu)$  is the subtraction constant evaluated at the renormalization scale  $\mu = 1$  GeV and will be determined so as to reproduce the experimental data. We take a common value for the  $K^+p$  and  $K^+n$  channels. The nucleon and kaon masses,  $M_N$  and  $M_K$ , are taken at their isospin averaged physical values. The kinematical parameter  $\bar{q}$  is the magnitude of the 3-momentum in the c.m. system. Thus, the unitarized amplitudes are given by

$$f_{\text{uni}}^I = \sum_{l=0}^{\infty} [(l+1)\mathcal{T}_{l+}^I + l\mathcal{T}_{l-}^I] P_l(\cos \theta_{\text{c.m.}}), \quad (50)$$

$$g_{\text{uni}}^I = \sum_{l=1}^{\infty} [\mathcal{T}_{l+}^I - \mathcal{T}_{l-}^I] \sin \theta_{\text{c.m.}} \frac{dP_l(\cos \theta_{\text{c.m.}})}{d \cos \theta_{\text{c.m.}}}. \quad (51)$$

## 4. Numerical result

### 4.1. $K^+N$ amplitude

In the previous section, we have calculated the tree level  $K^+N$  amplitude based on chiral perturbation theory up to the next-to-leading order. In this section, we carry out the  $\chi^2$  fitting to the experimental data to determine the low energy constants. We use the experimental data of the  $K^+p$  and  $K^+n$  elastic differential cross sections.

**Table 1** Determined parameters for the tree and unitarized amplitudes. The middle column shows the parameters of the tree amplitude and the right column is for the unitarized amplitude.  $b_0^{I=0}$  can be fixed by  $b^{I=1}$ ,  $b_0$  and  $b_F$ .

parameter	tree level amplitude		unitarized amplitude	
$b^{I=1}$	$1.01 \times 10^{-5} \text{ MeV}^{-1}$		$6.18 \times 10^{-4} \text{ MeV}^{-1}$	
$d^{I=1}$	$4.33 \times 10^{-4} \text{ MeV}^{-1}$	$\chi^2/N = 0.83$	$3.00 \times 10^{-4} \text{ MeV}^{-1}$	$\chi^2/N = 0.68$
$a$			$-1.224$	
$b^{I=0}$	$-2.69 \times 10^{-4} \text{ MeV}^{-1}$		$3.39 \times 10^{-4} \text{ MeV}^{-1}$	
$d^{I=0}$	$9.11 \times 10^{-4} \text{ MeV}^{-1}$	$\chi^2/N = 0.85$	$-9.15 \times 10^{-4} \text{ MeV}^{-1}$	$\chi^2/N = 1.02$

We use the isospin averaged masses of nucleon, kaon,  $\Lambda$  and  $\Sigma$  and the meson decay constants [27] as

$$M_N = 938.9 \text{ MeV}/c^2, \quad (52)$$

$$M_K = 495.6 \text{ MeV}/c^2, \quad (53)$$

$$M_\Lambda = 1193.2 \text{ MeV}/c^2, \quad (54)$$

$$M_\Sigma = 1115.7 \text{ MeV}/c^2, \quad (55)$$

$$f_K = (1.19 \pm 0.01)f_\pi = 110 \text{ MeV} \quad (56)$$

with  $f_\pi=92.4 \text{ MeV}$ . The values of the low energy constants  $D$  and  $F$  in the leading order chiral Lagrangian are determined by the fit to the data of the semileptonic hyperon decay as reported in Ref. [28]:

$$D = 0.80, \quad F = 0.46. \quad (57)$$

The low energy constants  $b_D$  and  $b_F$  can be determined by the baryon masses using Eqs. (17) to (20). These parameters shift the chiral limit baryon mass  $M_0$  to their physical masses. Using the isospin averaged masses, we have

$$b_D = \frac{3(M_\Sigma - M_N)}{16M_K^2} \frac{1 + \frac{\hat{m}}{m_s}}{1 - \frac{\hat{m}}{m_s}} = 2.10 \times 10^{-4} \text{ MeV}^{-1}, \quad (58)$$

$$b_F = -\frac{M_\Xi - M_N}{8M_K^2} \frac{1 + \frac{\hat{m}}{m_s}}{1 - \frac{\hat{m}}{m_s}} = 6.90 \times 10^{-5} \text{ MeV}^{-1} \quad (59)$$

with

$$\frac{\hat{m}}{m_s} = \frac{M_\pi^2}{2M_K^2 - M_\pi^2} = 0.040. \quad (60)$$

The rest of the low energy constants are determined so as to reproduce the observed cross section by using the  $\chi^2$  fit. The value of  $\chi^2$  is given by

$$\chi^2 = \sum_i^N \left( \frac{y_i - f(x_i)}{\sigma_i} \right)^2 \quad (61)$$

where  $y_i$ ,  $f(x_i)$ ,  $\sigma_i$  and  $N$  are the experimental data, the theoretical calculations which include the parameters, the errors of the data and the number of the data, respectively. We

use the partial wave series up to the  $G$ -wave ( $l = 4$ ), and we have confirmed the convergence of the partial wave expansion. In the isospin basis, we define

$$b^{I=1} = b_0 + b_D, \quad (62)$$

$$d^{I=1} = 2d_2 + d_3 + d_4, \quad (63)$$

$$b^{I=0} = b_0 - b_F, \quad (64)$$

$$d^{I=0} = 2d_1 - 2d_4 + d_3. \quad (65)$$

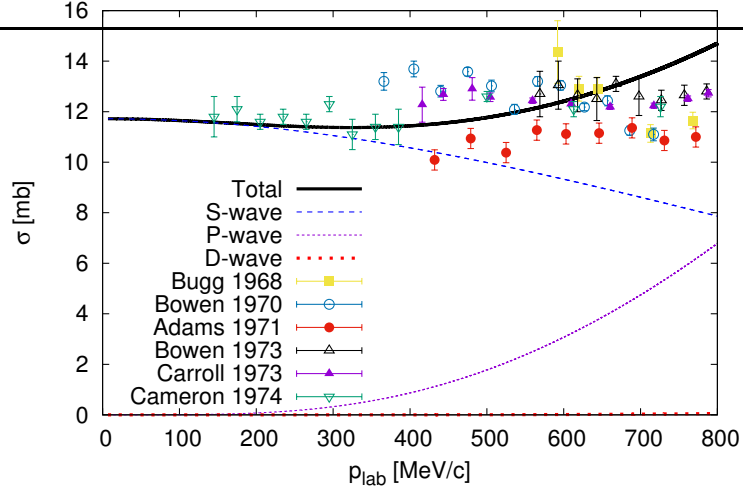
First, to determine the the low energy constants for  $I = 1$ ,  $b^{I=1}$ ,  $d^{I=1}$ , we carry out the  $\chi^2$  fit for the  $K^+p$  elastic differential cross section using the data at the laboratory momentum  $p_{\text{lab}} = 205 \text{ MeV/c}$  ( $N=21$ ) [30] where chiral perturbation theory may be applicable. The best fit of the parameters for  $K^+p$  is summarized in the middle column of Table 1. At this time, we can determine  $b_0$  from  $b^{I=1}$  with Eq. (62) as  $b_0 = -2.00 \times 10^{-4} \text{ MeV}^{-1}$ . Using the values of  $b_0$  and  $b_F$ , the parameter  $b^{I=0}$  is calculated by Eq. (64) in Table 1. Then, we carry out the  $\chi^2$  fit for  $K^+n$  elastic differential cross section to determine only  $d^{I=0}$  using the data at the  $p_{\text{lab}} = 434 \text{ MeV/c}$  ( $N=10$ ) [31]. The best fit of the parameters for  $I = 0$  is found in Table 1.

In the following, we compare our results with the experimental values for energies up to 800 MeV/c, from which inelastic contributions like pion production start to be significant. In Figs. 3 and 4, we show the results of the total cross sections calculated with the tree level amplitude, obtained by chiral perturbation theory up to the next-to-leading order. In spite of the perturbative calculation, we find substantially nice agreement with the data up to  $p_{\text{lab}} = 600 \text{ MeV/c}$ . It is also found that the contribution of the partial wave series up to the  $P$ -wave is dominant. In Fig. 5, we show the differential cross section of the  $K^+p$  elastic scattering together with the experimental data [30]. In the theoretical calculation, we include the Coulomb correction discussed in Sec. 3.2. Although we have used only the data at  $p_{\text{lab}} = 205 \text{ MeV/c}$  to determine the parameters, surprisingly we obtain great reproduction of the differential cross sections for lower and higher energies up to the  $p_{\text{lab}} = 500 \text{ MeV/c}$ . In Fig. 6, we show the differential cross section of the  $K^+n$  elastic cross section at the  $p_{\text{lab}} = 434$  and 526 MeV/c with the experimental data taken from Refs. [31]. Although we reproduce well  $I = 0$  total cross section in the low energy region with the parameter determined by  $K^+n$  differential cross section at  $p_{\text{lab}} = 434 \text{ MeV/c}$  as shown in Fig. 4, the reproduction of the  $K^+n$  differential cross section at  $p_{\text{lab}} = 526 \text{ MeV/c}$  is not so impressive.

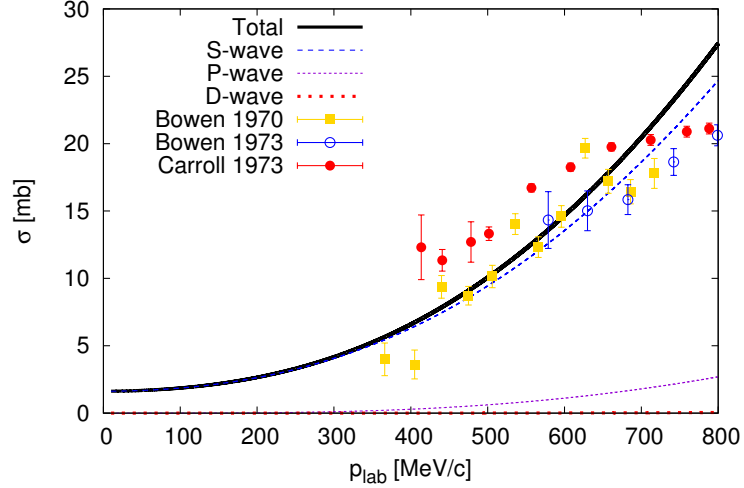
#### 4.2. Wavefunction renormalization

We have obtained a good description of the  $K^+N$  amplitude in the low energies. In this subsection, we calculate the wavefunction renormalization using the amplitude calculated above by following the method summarized in Sec. 2. The self-energy of  $K^+$  in the nuclear medium is calculated by Eq. (2) with the forward  $KN$  elastic amplitude by taking account of the Fermi motion of the nucleons. We assume symmetric nuclear matter and evaluate the wavefunction renormalization at the saturation density  $\rho_0$ . For symmetric nuclear matter, we consider the averaged amplitude of the  $K^+p$  and  $K^+n$  elastic scattering, which is given in terms of the isospin amplitudes by

$$T(\theta_{\text{c.m.}} = 0) = \frac{1}{4}[3T^{I=1}(\theta_{\text{c.m.}} = 0) + T^{I=0}(\theta_{\text{c.m.}} = 0)]. \quad (66)$$



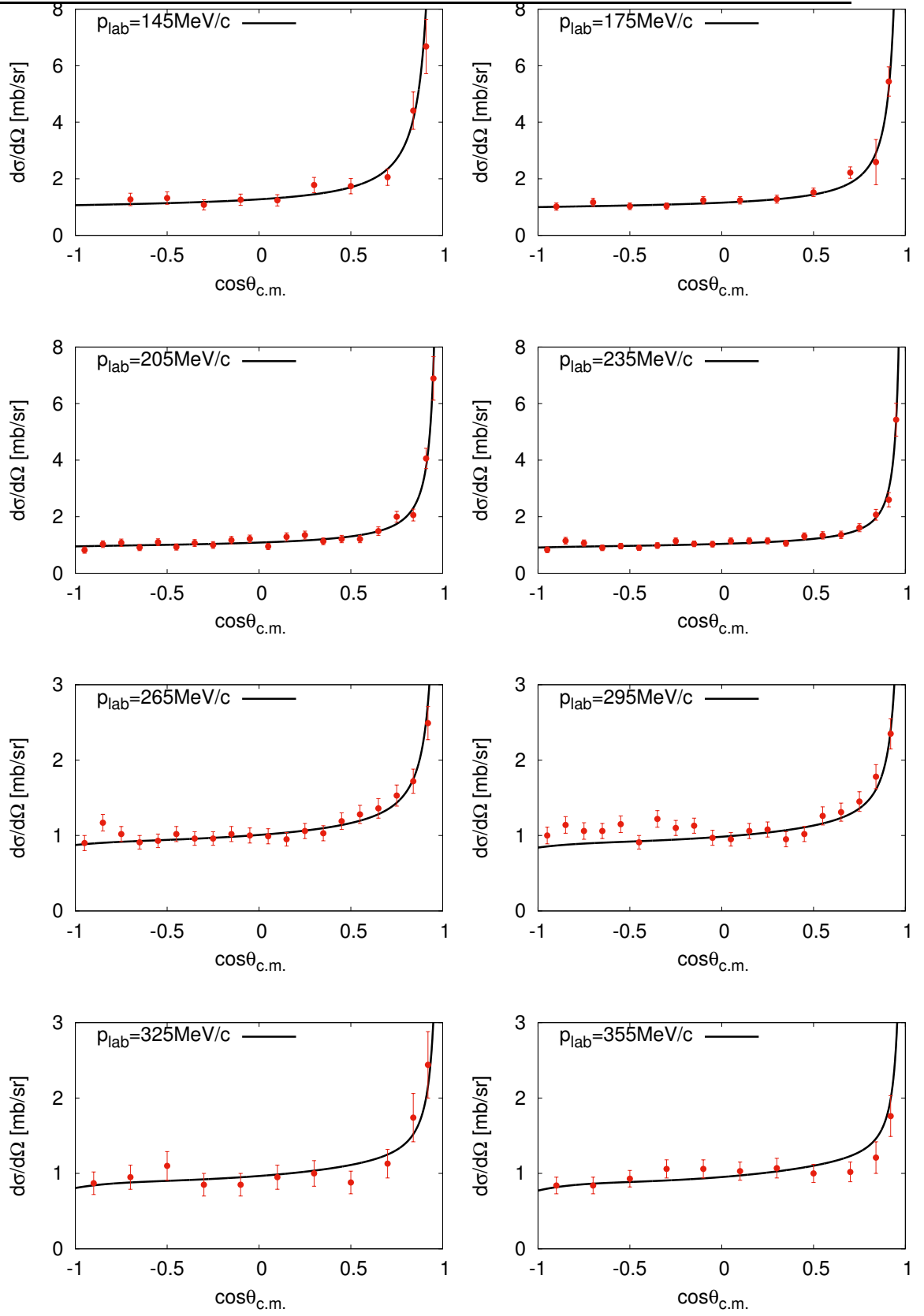
**Fig. 3** The  $I = 1$  total cross section from chiral perturbation theory up to the next-to-leading order comparison with the experimental data [30, 33–37]. The partial wave contributions are plotted in the dashed lines. The horizontal axis means the  $K^+$  meson incident momentum in the lab frame  $p_{\text{lab}}$  in the unit of MeV/c and the vertical axis means the total cross section  $\sigma$  in the unit of mb.



**Fig. 4** The  $I = 0$  total cross section from chiral perturbation theory up to the next-to-leading order comparison with the experimental data [33–35].

Before going into the numerical calculation, we show a simple analytic calculation, which is good to illustrate the method of the wavefunction renormalization [19]. We consider the model-independent Weinberg-Tomozawa term at tree level which is leading order chiral perturbation theory. The Weinberg-Tomozawa term is given by

$$T_{WT}^{I=0} = 0, \quad T_{WT}^{I=1} = \frac{1}{2f_K^2} \bar{u}(\vec{p}_4, s) (\not{p}_1 + \not{p}_3) u(\vec{p}_2, s) \quad (67)$$



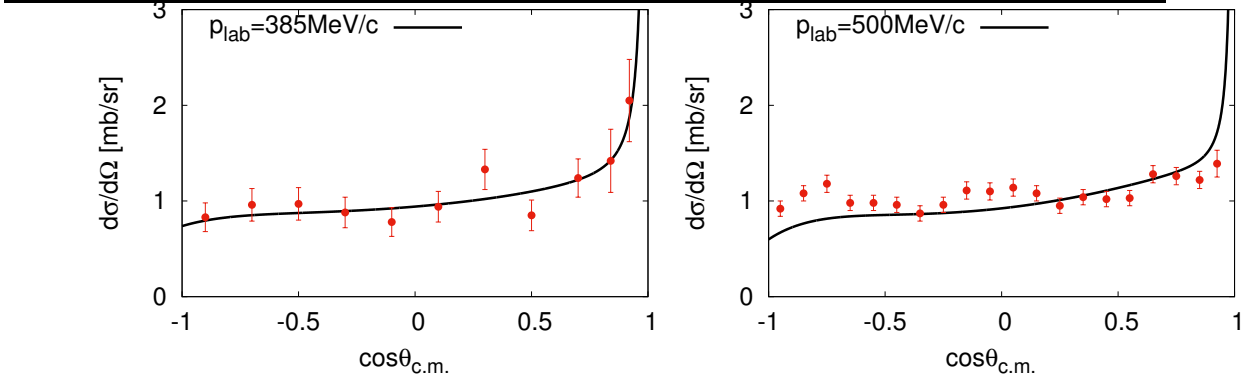


**Fig. 5** The differential cross section of  $K^+p$  elastic scattering at several lab momentum  $p_{\text{lab}}$  compared with the experimental data of Ref. [30]. The differential cross section  $d\sigma/d\Omega$  is shown in units of mb/sr as a function of  $\cos\theta_{\text{c.m.}}$ .

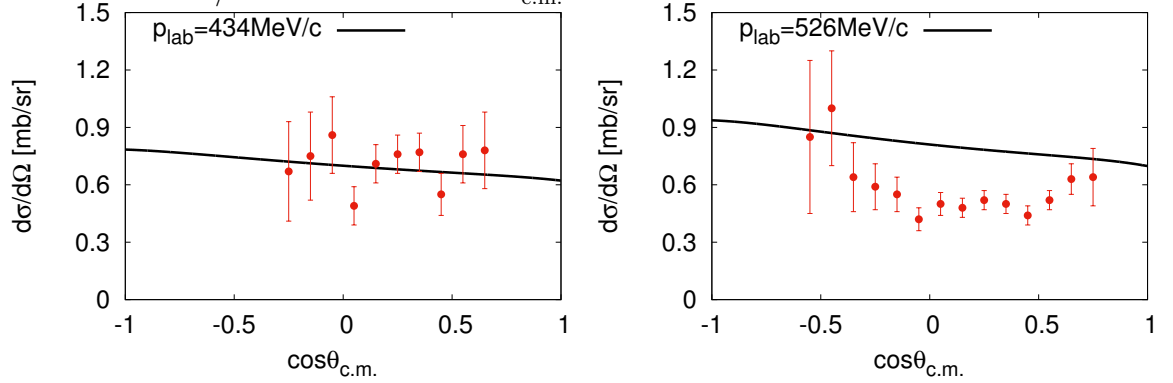


**Fig. 6** The differential cross section of  $K^+n$  elastic scattering compared with the experimental data of Ref. [31].

as we saw in Sec. 3. The isospin averaged tree level forward amplitude for Weinberg-Tomozawa term is given by

$$T(\theta_{\text{c.m.}} = 0) = \frac{3}{4} \frac{\omega^*}{f_K^2}. \quad (68)$$

Using Eq. (68), we calculate the wavefunction renormalization factor  $Z$  at the threshold  $\omega^* = M_K$  without Fermi motion using Eqs. (3) and (6)

$$\begin{aligned} Z &= 1 + \frac{3\rho_0}{8M_K f_K^2} \frac{\rho}{\rho_0} \\ &= 1 + 0.082 \frac{\rho}{\rho_0}. \end{aligned} \quad (69)$$

This result means that the magnitude of the amplitude is increased by about 8% at the saturation density due to the wavefunction renormalization.

Now let us show the wavefunction renormalization factor obtained from the  $K^+N$  scattering calculated by chiral perturbation theory up to the next-to-leading order. The results for the wavefunction renormalization factor are summarized in Table 2. In the middle columns,

**Table 2** The wavefunction renormalization factor without the Fermi motion  $Z_{w/o}$  and with the Fermi motion  $Z$  obtained by chiral perturbation theory up to the next-to-leading order.  $p_{K^+}$  is the  $K^+$  momentum at the nuclear matter rest frame. The  $K^+$  energy is given by  $E_{K^+} = \sqrt{p_{K^+}^2 + M_K^2}$ .

$p_{K^+}$ [MeV/c]	$Z_{w/o}$	$Z$
0.0	1.08	1.08
130.0	1.08	1.08
488.0	1.06	1.06
531.0	1.05	1.06
656.0	1.05	1.05
714.0	1.04	1.05

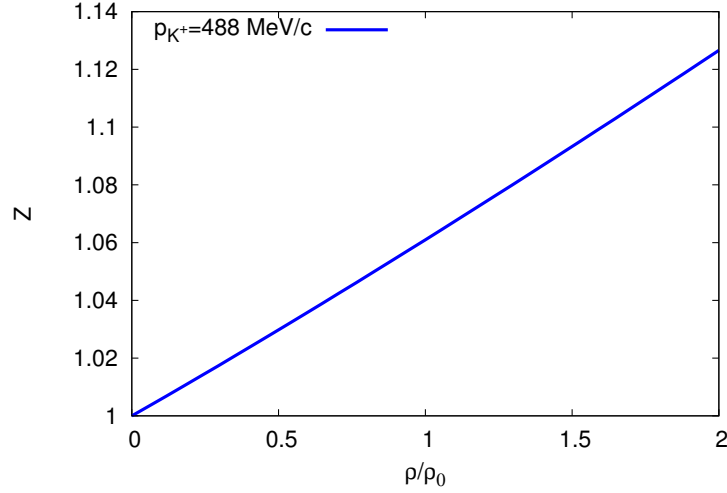


**Fig. 7** The density dependence of the wavefunction renormalization factor  $Z$  with Fermi motion at the  $p_{K^+} = 488$  MeV/c using the tree level amplitude.

we show the results without Fermi motion of the nucleons which is calculated by Eq. (2), while in the right columns we have the results the Fermi motion calculated by Eq. (3). The table shows that the wavefunction renormalization factor gives 5 to 8% enhancement for the in-medium self-energy at the saturation density. This shows that the wavefunction renormalization could explain a part of the breakdown of the linear density approximation for the  $K^+$ -nucleus scattering. We also find in Table 2 that the effect of the Fermi motion for the nucleons is minor. In Fig. 7, we show also the density dependence of the wavefunction renormalization factor with the Fermi motion at the  $p_{K^+} = 488$  MeV/c. Because of the minor contribution of the Fermi motion, the density dependence is almost linear in this approximation. For further detailed study of the medium effects on  $K^+$ , we need to develop in-medium chiral perturbation theory for the  $K$  meson similar for the pion developed, for example, in Refs. [38, 39].



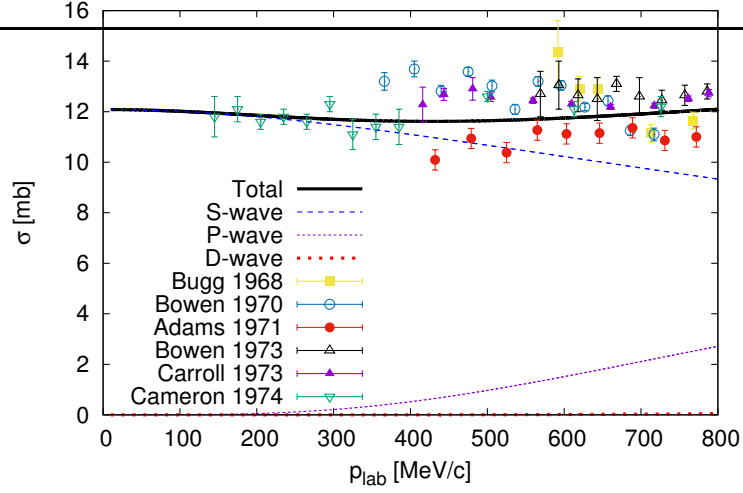
#### 4.3. Unitarized amplitude and possible resonance in $I = 0$

To compare the tree level amplitude with the unitarized amplitude, we also carry out the  $\chi^2$  fit for the unitarized  $I = 0$  and 1 amplitudes. First, to determine the the low energy constants for  $I = 1$ ,  $b^{I=1}$ ,  $d^{I=1}$  and the subtraction constant  $a$ , we carry out the  $\chi^2$  fit for  $K^+p$  elastic differential cross section using the data at the  $p_{\text{lab}} = 726$  MeV/c ( $N=20$ ) [30] where  $P$ -wave contribution is well constrained. In the point of view of chiral perturbation theory, one may think that the momentum  $p_{\text{lab}} = 726$  MeV/c would be out of applicable energies of chiral perturbation theory, while carrying out unitarization makes applicable region wider. The best fit of the parameters for  $K^+p$  is summarized in the right column of Table 1. At this time, we can determine  $b_0$  from  $b^{I=1}$  with Eq. (62) as  $b_0 = 4.08 \times 10^{-4}$  MeV $^{-1}$ . Using the values of  $b_0$  and  $b_F$ , the parameter  $b^{I=0}$  is calculated by Eq. (64) as shown in Table 1. Then, we carry out the  $\chi^2$  fit for  $K^+n$  elastic differential cross section to determine  $d^{I=0}$  using the data at the  $p_{\text{lab}} = 720$  MeV/c ( $N=18$ ) [32]. The best fit of the parameters for  $I = 0$  is found in the right column of Table 1.

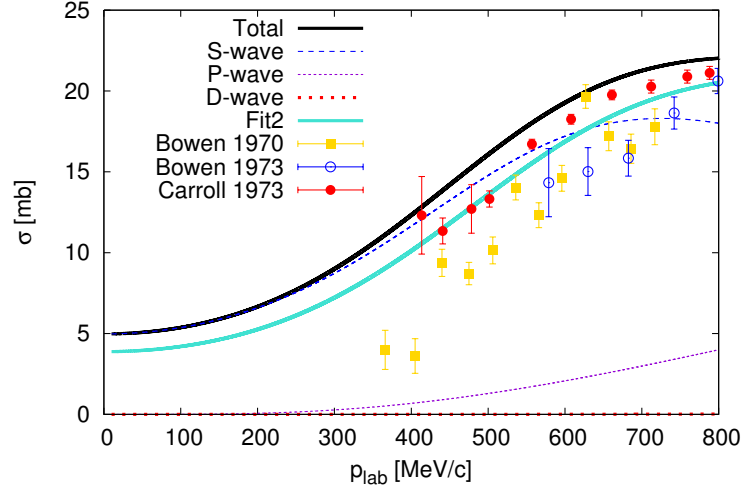
In the following, we compare our results with the experimental values. The results for the total cross section are shown in Figs. 8 and 9. In the result for  $I = 0$ , the calculated cross section is a bit overestimated than the experimental data. As a comparative study, we also determine the  $I = 0$  parameter using the data of the total cross section at  $p_{\text{lab}} = 336$  to 799 MeV/c ( $N = 27$ ) [33–35]. The best value of the parameter is obtained as  $d^{I=0} = -8.86 \times 10^{-4}$  MeV $^{-1}$  with  $\chi^2/N = 6.85$ . This value is very similar with the one which we have determined with the data of the differential cross section at  $p_{\text{lab}} = 720$  MeV/c. In Fig. 9, we also plot the total cross section calculated with this parameter as “Fit2” to referred, and we find that the agreement between the theoretical calculation and the experimental data is improved, but there is no significant difference between two theoretical results and essentially these two are the same result.

In Fig. 10, we show the differential cross section of the  $K^+p$  elastic scattering together with the experimental data [30]. Although we have used only the data at  $p_{\text{lab}} = 726$  MeV/c to determine the parameters, surprisingly we obtain great reproduction of the differential cross sections for lower energies. In Fig. 11, we show the differential cross section of the  $K^+n$  elastic cross section with the experimental data taken from Refs. [31, 32]. Although having determined the parameter using only the data at  $p_{\text{lab}} = 720$  MeV/c, we find fairly nice reproduction in other lower momenta. Especially, for  $p_{\text{lab}}=640, 720$  and 780 MeV/c, the agreement between the calculation and data is quite good both in magnitude and angular dependence. These data are from the same experiment [32]. For the other lab momenta, which are from different experiment [31], the agreement is marginal especially for lower energies. We can use these data to determine the parameter and find a solution which provides a much better reproduction for the differential cross sections, but with this solution we cannot reproduce the  $I = 0$  total cross section.

Then, we calculate the wavefunction renormalization factor  $Z$  for the unitarized amplitude. The results with Fermi motion are found in the Table. 3 and Fig. 12. Contrary to our expectation, in low momenta, our calculation shows that the magnitude of the wavefunction renormalization factor at the saturation density gets smaller than unity as seen in Table 3. In Fig. 12, we compare the  $K^+$  momentum dependence of the wavefunction renormalizations calculated by the tree amplitude and the unitarized amplitude. As seen in the figure, the

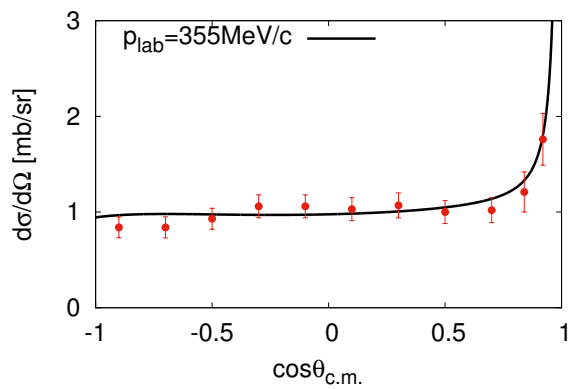
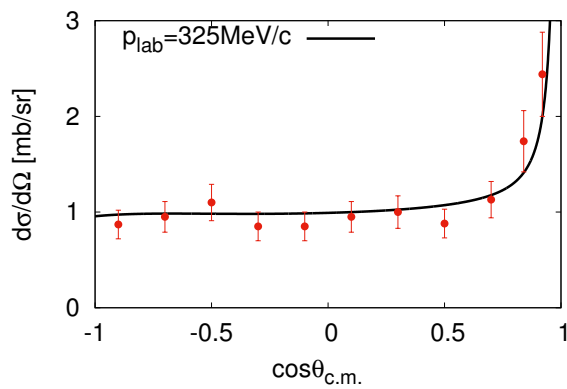
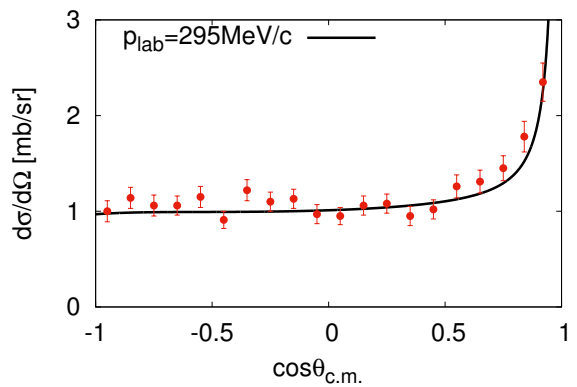
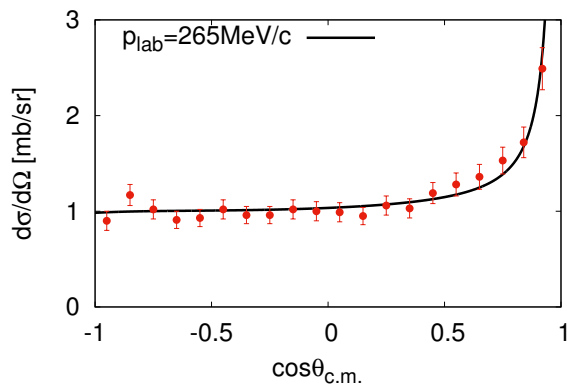
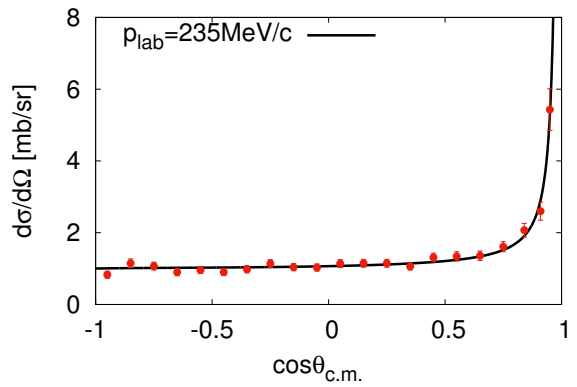
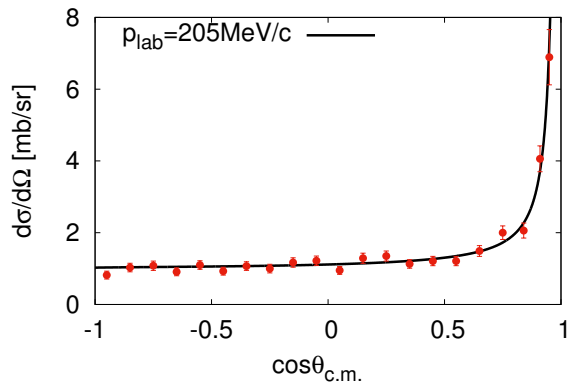
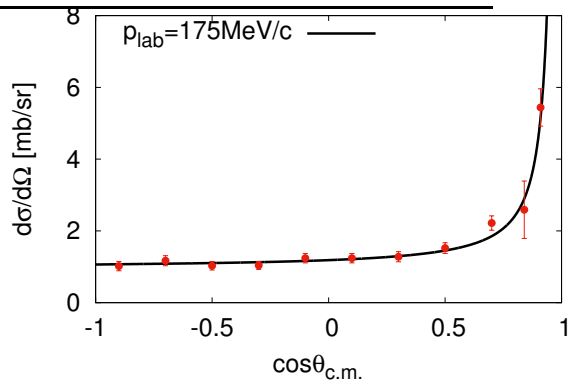
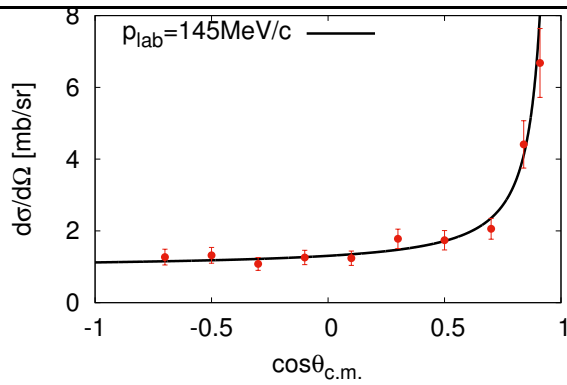


**Fig. 8** The  $I = 1$  total cross section from unitarization comparison with the experimental data [30, 33–37].



**Fig. 9** The  $I = 0$  total cross section from unitarization comparison with the experimental data [33–35]. The upper solid line “Total” is correspond to the value of Table 1 and the lower solid line “Fit2” is correspond to the value determined by the  $I = 0$  total cross section.

wavefunction renormalization obtained by the tree amplitude monotonously decreases as the  $K^+$  momentum increases, while the one calculated by the unitarized amplitude drastically depends on the  $K^+$  momentum and has some structure. In particular it crosses unity around  $p_{K^+} = 600$  MeV/c. Because the wavefunction renormalization factor is calculated by derivative of the scattering amplitude, the fact that  $Z$  has nontrivial energy dependence implies that the scattering amplitude also should have nontrivial structure. In Fig. 13, we show the unitarized amplitude of the  $S$ -wave  $KN$  scattering in the  $I = 0$  channel. This figure shows that the imaginary part has rapid increase around  $p_{\text{lab}} = 500$  MeV/c, which correspond to  $E_{\text{c.m.}} = 1565$  MeV, and the real part has a peak at the same point. One naturally expects that this kind of structure stems from a pole of the amplitude in the complex energy plane.



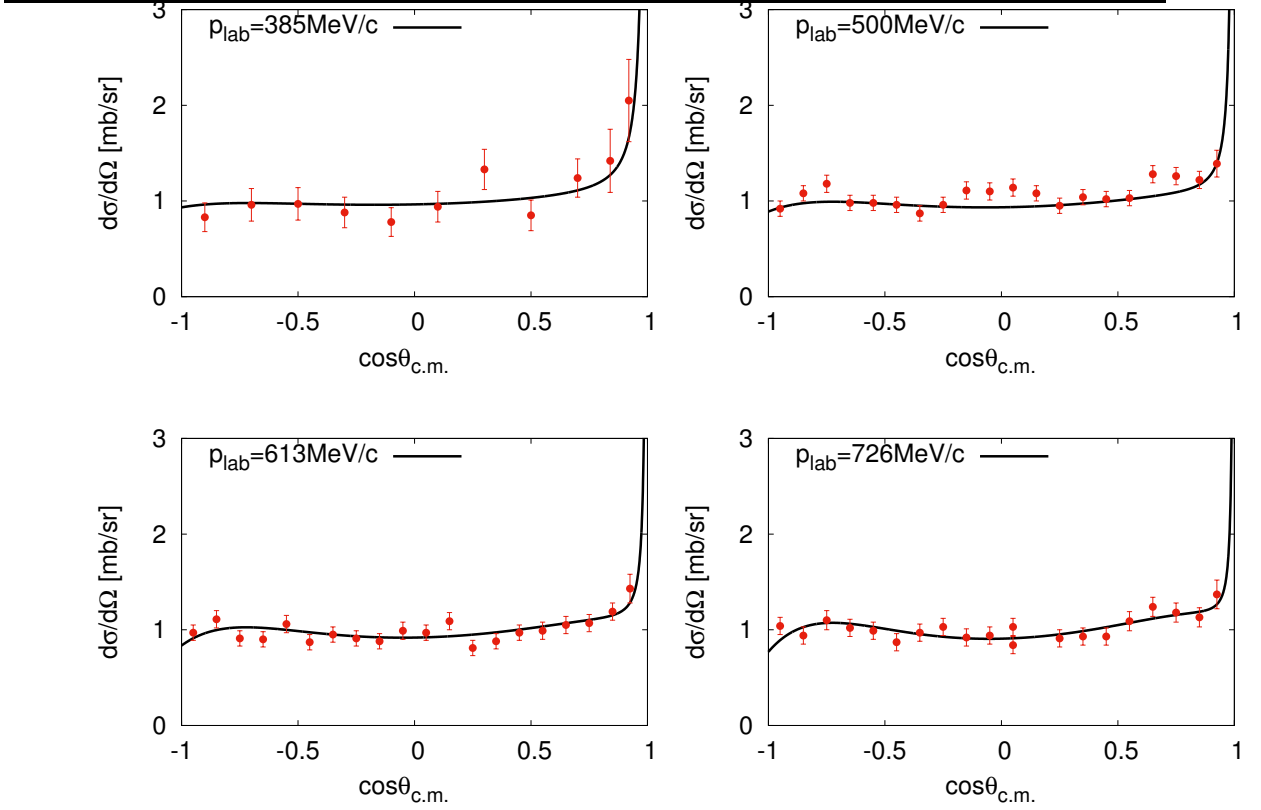


**Fig. 10** The differential cross section of  $K^+p$  elastic scattering at several lab momentum  $p_{\text{lab}}$  compared with the experimental data of Ref. [30].

Actually, we look for a pole of the  $S$ -wave amplitude with  $I = 0$  in the second Riemann sheet of the complex energy plane, and we find a pole at  $E_{\text{c.m.}} = 1562 - 219i$  MeV.

This pole of the scattering amplitude may represent a hadronic resonance with spin-parity  $J^P = \frac{1}{2}^-$ , strangeness  $S = +1$  and isospin  $I = 0$ . This resonance is dynamically generated by the  $KN$  scattering with the subtraction constant close to the natural value  $a = -1.024$  for  $\mu = 1$  GeV [40], which means that the resonance is constructed almost purely by the hadronic components, the  $K$  meson and the nucleon, without other components such as quark components. This resonance is certainly different from the so-called pentaquark suggested by the LEPS group [41], because our resonance has a very large width. We find also that the driving force to form the  $KN$  resonance is attractive contribution from the next-to-leading order terms, while the leading order Weinberg-Tomozawa term is null for the  $KN$  channel with  $I = 0$ . Hence, this resonance is not contradict to the argument of Refs. [42, 43], in which it is concluded that exotic channels cannot produce dynamical resonance of meson and baryon. The details of this resonance will be discussed somewhere [44].

The wavefunction renormalization obtained by the unitarized amplitude explains only a few percent of the enhancement in the optical potential around  $p_{K^+} > 600$  MeV/c. The unitarized amplitude might not be realistic to describe the  $K^+N$  scattering. Nevertheless, what we have learn in this study is that if the wavefunction renormalization factor crosses unity at a certain momentum, the scattering amplitude should have strong energy dependence, which

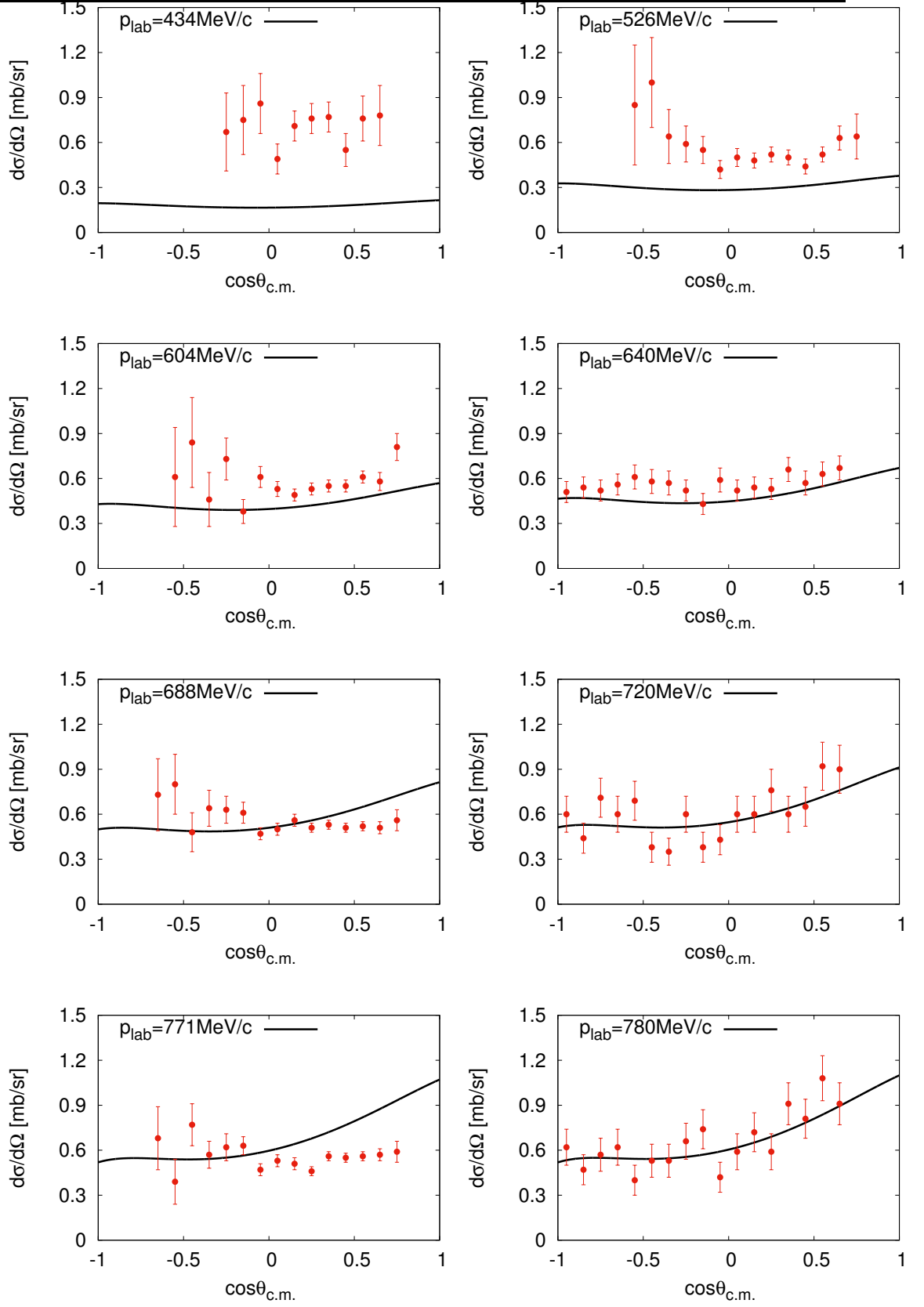


**Fig. 11** The differential cross section of  $K^+n$  elastic scattering compared with the experimental data of Ref. [31, 32]. The momenta at the  $p_{\text{lab}}=640, 720$  and  $780$  MeV/c are the data from Ref. [32]. The others are the data from Ref. [31].

**Table 3** The wavefunction renormalization factor with the Fermi motion  $Z$  obtained by the unitarized amplitude.

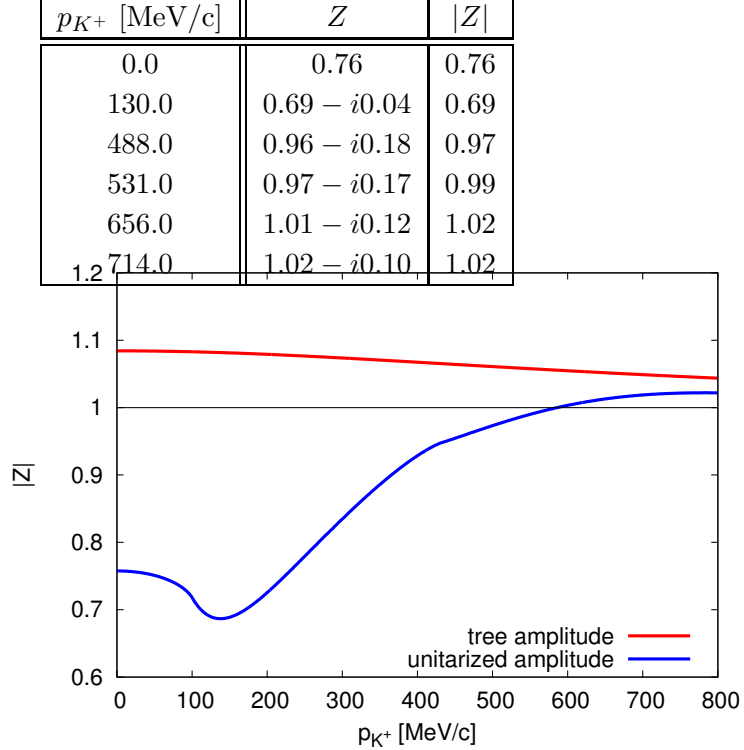


**Fig. 12** The kaon momentum dependence of the wavefunction renormalization factors  $Z$  with Fermi motion obtained by the tree level amplitude and unitarized amplitude.

could stem from the presence of a resonance. Thus, because the wavefunction renormalization factor has direct information of the scattering amplitude, observing the momentum dependence of the  $K^+$  wavefunction renormalization factor in nuclear matter could provide a hint of the existence of an exotic hadron with  $S = +1$ .

## 5. Sumarry and Conclusion

We have calculated the wavefunction renormalization to explain a part of the “missing” repulsion of the  $K^+N$  interaction in-medium. This study is one of the first steps to reveal the in-medium  $K^+N$  interaction in the context of the partial restoration of chiral symmetry. The wavefunction renormalization is a next-to-leading order correction on the  $K^+$  self-energy in the density expansion, but the leading order correction on in-medium  $K^+N$  scattering. In this paper, we have done the following procedure to calculate the wavefunction renormalization; we have calculated the in-vacuum  $K^+N$  interaction in chiral perturbation theory up to the next-to-leading order. We have determined the low energy constants by carrying out the  $\chi^2$  fits so as to reproduce the  $K^+N$  scattering cross section. Using the constructed  $K^+N$  amplitude, we have calculated the wavefunction renormalization by taking

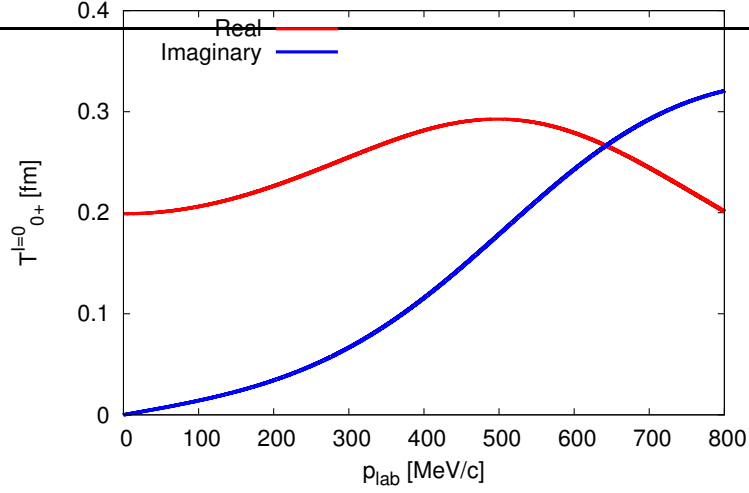


**Fig. 13** The unitarized amplitude of the  $S$ -wave  $KN$  scattering in the  $I = 0$  channel  $\mathcal{T}_{0+}^{I=0}$  as the function of kaon lab momentum  $p_{\text{lab}}$ . It shows that the real part and the imaginary part of  $\mathcal{T}_{0+}^{I=0}$ .

the energy-derivative of the  $K^+$  self-energy in the nuclear medium. The self-energy is calculated in the Thomas-Fermi approximation. We have obtained quite good  $K^+p$  amplitude which reproduces the differential cross sections below  $p_{\text{lab}} = 500$  MeV/c, although the fitting was performed only at  $p_{\text{lab}} = 205$  MeV/c. The reproduction of the  $I = 0$  total cross section is also satisfying.

We have found that the wavefunction renormalization factor at the saturation density is about 5 to 8% depending on the kaon momentum. This implies that the  $K^+N$  interaction gets 5 to 8% enhancement in nuclear matter. It shows that the wavefunction renormalization explains a part of the enhancement of the  $K^+N$  interaction in nuclear medium and hence is one of the important medium effects for the in-medium  $K^+$ . We have also found that the wavefunction renormalization factor gets decreasing when the kaon momentum increases.

For comparison, we have used chiral perturbation theory up to the next-to-leading order and we have carried out the unitarization of the amplitude obtained by chiral perturbation theory. We have determined the low energy constants and subtraction constant by carrying out the  $\chi^2$  fits so as to reproduce the observable. We have obtained the better reproduction of the  $I = 0$  and 1 total and differential cross section in the higher energies compared with the tree amplitude. The behavior of the wavefunction renormalization obtained by the unitarized amplitude is quite different to the one obtained by the tree level amplitude. In the low energies, the wavefunction renormalization factor has the values below unity. This behavior might be responsible for the dynamically generated resonance of the  $S$ -wave  $KN$  scattering in the  $I = 0$  channel. Investigating the momentum dependence of the wavefunction renormalization factor could reveal the existence of an  $S = +1$  resonance.

As the future prospects, we will take into account other in-medium effects than the wavefunction renormalization, such as mass modification and vertex correction. Such effects are systematically taken into account by considering the in-medium chiral perturbation theory. For this purpose, we will need to construct a theoretical framework of the 3-flavor

---

in-medium chiral perturbation theory. With this approach, we will reveal the behavior of the wavefunction renormalization when other in-medium effects are considered.

## Acknowledgment

The work of D.J. was partly supported by Grants-in-Aid for Scientific Research from JSPS (25400254, 17K05449).

## References

- [1] K. Suzuki *et al.*, Phys. Rev. Lett. **92**, 072302 (2004).
- [2] E. Friedman *et al.*, Phys. Rev. Lett. **93**, 122302 (2004).
- [3] E. E. Kolomeitsev, N. Kaiser and W. Weise, Phys. Rev. Lett. **90**, 092501 (2003).
- [4] D. Jido, T. Hatsuda and T. Kunihiro, Phys. Lett. B **670**, 109 (2008).
- [5] C. B. Dover and G. E. Walker, Phys. Rept. **89**, 1 (1982).
- [6] As a recent review, T. Hyodo and D. Jido, Prog. Part. Nucl. Phys. **67**, 55 (2012).
- [7] D. V. Bugg *et al.*, Phys. Rev. **168** 1466 (1968).
- [8] W. Weise, Nuovo Cim. A **102**, 265 (1989).
- [9] R. A. Krauss *et al.*, Phys. Rev. C **46**, 655 (1992).
- [10] E. Friedman and A. Gal, Phys. Rept. **452**, 89 (2007).
- [11] P. B. Siegel, W. B. Kaufmann and W. R. Gibbs, Phys. Rev. C **31**, 2184 (1985).
- [12] R. J. Peterson, Phys. Rev. C **60**, 022201 (1999).
- [13] G. E. Brown, C. B. Dover, P. B. Siegel and W. Weise, Phys. Rev. Lett. **60**, 2723 (1988).
- [14] M. F. Jiang and D. S. Koltun, Phys. Rev. C **46**, 2462 (1992).
- [15] C. Garcia-Recio, J. Nieves and E. Oset, Phys. Rev. C **51**, 237 (1995).
- [16] J. C. Caillon and J. Labarsouque, Phys. Rev. C **53**, 1993 (1996).
- [17] E. Friedman, Nucl. Phys. A **954**, 114 (2016).
- [18] E. Friedman, EPJ Web Conf. **130**, 02005 (2016).
- [19] D. Jido, arXiv:1603.07083 [nucl-th].
- [20] D. Jido, T. Hatsuda and T. Kunihiro, Phys. Rev. D **63**, 011901 (2001).
- [21] N. Kaiser, P. B. Siegel and W. Weise, Nucl. Phys. A **594** 325 (1995).
- [22] E. Oset and A. Ramos, Nucl. Phys. A **635**, 99 (1998).
- [23] E. Oset, A. Ramos and C. Bennhold, Phys. Lett. B **527**, 99 (2002).
- [24] K. Hashimoto, Phys. Rev. C **29**, 1377 (1984).
- [25] D. Jido, E. Oset and A. Ramos, Phys. Rev. C **66**, 055203 (2002).
- [26] J. A. Oller and E. Oset, Phys. Rev. D **60**, 074023 (1999).
- [27] C. Patrignani *et al.* (Particle Data Group), Chin. Phys. C, **40**, 100001 (2016).
- [28] M. A. Luty and M. J. White, Phys. Lett. B **319**, 261 (1993).
- [29] Y. Ikeda, T. Hyodo and W. Weise, Phys. Lett. B **706**, 63 (2011).
- [30] W. Cameron *et al.*, Nucl. Phys. B **78**, 93 (1974).
- [31] C. J. S. Damerell *et al.*, Nucl. Phys. B **94**, 374 (1975).
- [32] G. Giacomelli *et al.*, Nucl. Phys. B **56** 346 (1973).
- [33] T. Bowen *et al.*, Phys. Rev. D **2**, 2599 (1970).
- [34] T. Bowen *et al.*, Phys. Rev. D **7**, 22 (1973).
- [35] A. S. Carroll *et al.*, Phys. Lett. **45B**, 531 (1973).
- [36] D. V. Bugg *et al.*, Phys. Rev. **168**, 1466 (1968).
- [37] C. J. Adams *et al.*, Phys. Rev. D **4**, 2637 (1971).
- [38] S. Goda and D. Jido, Phys. Rev. C **88**, no. 6, 065204 (2013).
- [39] S. Goda and D. Jido, PTEP **2014**, no. 3, 033D03 (2014).
- [40] T. Hyodo, D. Jido and A. Hosaka, Phys. Rev. C **78**, 025203 (2008).
- [41] T. Nakano *et al.*, Phys. Rev. Lett. **91**, 012002 (2003).
- [42] T. Hyodo, D. Jido, and A. Hosaka, Phys. Rev. Lett. **97** 192002 (2006).
- [43] T. Hyodo, D. Jido, and A. Hosaka, Phys. Rev. **D75** 034002 (2007).
- [44] K. Aoki, and D. Jido, in preparation.